

A mathematical model of the dynamics of the inner ear

By MARK H. HOLMES

Department of Mathematical Sciences, Rensselaer Polytechnic Institute,
Troy, New York 12181

(Received 2 March 1981 and in revised form 2 July 1981)

A three-dimensional hydroelastic model of the dynamical motion in the cochlea is analysed. The fluid is Newtonian and incompressible, and the basilar membrane is modelled as an orthotropic elastic plate. Asymptotic expansions are introduced, based on slender-body theory and the relative high frequencies in the hearing range, which reduce the problem to an eigenvalue problem in the transverse cross-section. After this, an example is worked out and a comparison is made with experiment and the earlier low-frequency theory.

1. Introduction

The problem of the high-frequency response of the cochlea has been studied rather extensively over the past few years. The primary reason is that the earlier theories are, seemingly, incapable of describing the rather sharp tuning present in the cochlea. In this paper a hydroelastic model of the dynamic response in the cochlea is proposed and then analysed for high, or at least moderately high, frequencies. Except for a few minor differences, the model is essentially the same as that used in Holmes (1981). One such difference is that the basilar membrane is now taken to be an orthotropic elastic plate. This assumption is made because of the fibre network present in the basilar membrane and is motivated by the observations of Voldrich (1978). The most important difference, however, is that certain adjustments are made in the asymptotics to account for the higher frequencies. This is, in fact, what distinguishes the present analysis from the earlier low-frequency theory.

In §§2 and 3 the problem is formulated and the underlying assumptions are presented. After this, the problem is reduced using a WKB type of approximation for a slender body. Aside from the differences mentioned earlier, this is essentially an extension of the approach used in the low-frequency theory. With it, the problem eventually reduces to a two-dimensional eigenvalue problem involving the fluid pressure and the displacement of the basilar membrane in the transverse cross-section. In §6, the reduced problem is solved by rewriting it, using a Green function, as an integro-differential equation for the displacement of the basilar membrane, and then expanding the solution in a Fourier series. Using the parameter values given in Holmes (1981), the resulting solution is shown to agree reasonably well, in the moderate- to high-frequency range, with experimental observations.

There are differences between our approach and almost every other model for the high-frequency response. For example, the problem treated here is fully three-dimensional, which distinguishes it from Lesser & Berkley (1972), Allen (1977) and de Boer (1979). These authors argue, justifiably, that two-dimensional systems are

more tractable and are, perhaps, the logical extension of the earlier long-wave theories. As stated above, with our approach, the problem also reduces to solving a two-dimensional system. The difference is that it is not in the longitudinal cross-section but, rather, in the transverse direction. Perhaps the two most important differences are that both the motion of the basilar membrane and the effects of the fluid viscosity are treated more carefully here. For example, it is almost universal to consider the motion of the basilar membrane as passive; i.e. to prescribe its motion in the formulation of the model. This has been done using impedance functions, as in the papers mentioned above, or by using a, presumably, first-term approximation of its deflection as in Steele & Taber (1979). Both of these assumptions go a long way in simplifying the problem but at the same time give rise to questions concerning their justifiability and/or consistency. In the analysis to follow, this difficulty does not occur as the motion of the basilar membrane is one of the principal components of the equations of motion. As a consequence of this, the following analysis is more general than the other theories.

2. Formulation of model

In what follows, the cochlea is idealized to consist of an unrolled tapered tube containing two chambers that are each filled with an incompressible viscous fluid (figure 1). The chambers are separated by a planar region, which contains a rigid section representing the bony shelf, and a flexible portion Γ representing the basilar membrane. At the apical end the two chambers are connected by an aperture in the partition, known as the helicotrema. The outer boundary of the cochlea consists of a rigid portion, called the cochlear wall, and two openings at the basal end that are each covered by a flexible membrane. The stapes transmits the signals from the outer ear to the cochlea by pushing against the upper opening Γ_w , which is known as the oval window. The lower opening, the round window, is represented by Γ_R . For simplicity, the cochlear wall is assumed to be symmetric through the (x, y) -plane. Also, away from the ends $x = 0, 1$ it is assumed that the boundary of the basilar membrane can be written as $y = G_{\pm}(x)$. The part of the boundary given by $y = G_+(x)$ represents the portion attached to the spiral lamina, and $y = G_-(x)$ is the portion attached to the spiral ligament.

The basilar membrane is modelled as a linear orthotropic elastic plate with a uniform thickness and which is simply supported along its boundary. The deflection of the plate is represented by $\eta(x, y, t)$.

The velocity and pressure of the fluid are represented by $\mathbf{v}(x, y, z, t)$ and $p(x, y, z, t)$, respectively. In what follows, both the dependent and independent variables are assumed to be dimensionless. Asterisks are used to indicate their dimensional analogues. So, for example, the non-dimensional spatial co-ordinates x, y, z are related to x^*, y^*, z^* as follows:

$$x^* = Lx, \quad y^* = By, \quad z^* = Bz,$$

where L and B are the length and width of the basilar membrane, respectively.

In non-dimensional form, the equations describing the motion are (Holmes 1981)

(i) for the fluid

$$\frac{\partial}{\partial t} \mathbf{v} - \delta^2 \left(\epsilon^2 \frac{\partial^2}{\partial x^2} + \frac{\partial^2}{\partial y^2} + \frac{\partial^2}{\partial z^2} \right) \mathbf{v} = -\nabla p, \quad (1a)$$

$$\epsilon^2 \frac{\partial}{\partial x} v_1 + \frac{\partial}{\partial y} v_2 + \frac{\partial}{\partial z} v_3 = 0; \quad (1b)$$

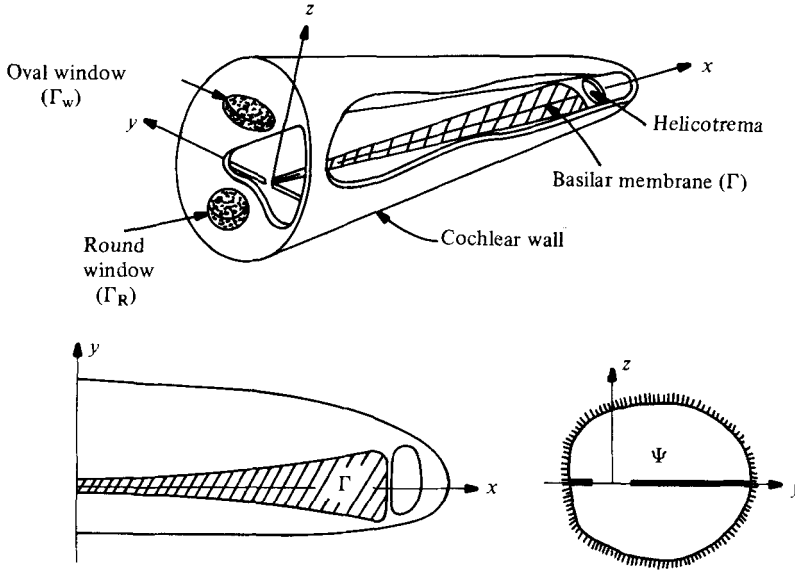


FIGURE 1. Geometry and notation for the hydroelastic model of the cochlea. Shown are a cutaway view of the cochlea, the plan form of the partition, and the transverse cross-section of the cochlea.

(ii) for the basilar membrane

$$\frac{\partial^4}{\partial y^4} \eta + 2\epsilon^2 D_3 \frac{\partial^4}{\partial x^2 \partial y^2} \eta + \epsilon^4 D_1 \frac{\partial^4}{\partial x^4} \eta + \frac{\epsilon^2}{\alpha} \frac{\partial^2}{\partial t^2} \eta = - \left[p + 2\delta^2 \frac{\partial}{\partial z} v_3 \right]_{\Gamma}. \quad (1c)$$

The parameters are

$$\epsilon = \frac{B}{L}, \quad \delta^2 = \frac{\nu}{B^2 \hat{\omega}_0}, \quad \alpha = \frac{\rho B}{\mu},$$

where ρ and ν represent the density and kinematic viscosity of the fluid, and μ is the mass density of the plate. Also,

$$\hat{\omega}_0^2 = \frac{D_2^*}{\rho L^2 B^3},$$

where D_2^* is the (dimensional) bending rigidity of the plate in the y -direction, and

$$[p]_{\Gamma} = p(x, y, 0^+, t) - p(x, y, 0^-, t).$$

The D_1 and D_3 in (1c) represent the respective bending and twisting rigidities normalized by D_2^* .

The fluid velocity satisfies the usual kinematic condition on the plate, i.e.

$$\mathbf{v}|_{\Gamma} = \left(0, 0, \epsilon^2 \frac{\partial}{\partial t} \eta \right). \quad (2)$$

Also, it satisfies the no-slip condition on the rigid portion of the cochlear wall and the bony shelf.

As a final comment on the notation, the cross-section of the upper chamber is represented by Ψ (figure 1). The boundary of Ψ , which is denoted by $\partial\Psi$, consists of a rigid section Σ , as well as the flexible portion from the basilar membrane which is represented by Γ_x .

3. Time-independent problem

We are interested, principally, in the longtime solution of the problem for a periodic forcing. Accordingly, it is assumed that

$$\mathbf{v} = \mathbf{u}(x, y, z) e^{i\omega t}, \quad p = \tilde{p}(x, y, z) e^{i\omega t}, \quad \eta = \zeta(x, y) e^{i\omega t}. \quad (3)$$

In §4, asymptotic expansions based on the smallness of the parameter ϵ are introduced. Since we are also concerned with the response for moderately high frequencies, we assume

$$\omega = \frac{\omega_0}{\epsilon}. \quad (4)$$

Also, owing to the small mass density of the basilar membrane

$$\alpha = \frac{\alpha_0}{\epsilon^2}. \quad (5)$$

With (3)–(5) the problem to be solved is given as follows:

$$i\omega_0 \mathbf{u} - \epsilon \delta^2 \nabla_\epsilon^2 \mathbf{u} = -\epsilon \nabla \tilde{p}, \quad (6a)$$

$$\epsilon^2 \frac{\partial}{\partial x} u_1 + \frac{\partial}{\partial y} u_2 + \frac{\partial}{\partial z} u_3 = 0, \quad (6b)$$

$$\left(\frac{\partial^4}{\partial y^4} + 2\epsilon^2 D_3 \frac{\partial^4}{\partial x^2 \partial y^2} + \epsilon^4 D_1 \frac{\partial^4}{\partial x^4} - \frac{\omega_0^2}{\alpha_0} \epsilon^2 \right) \zeta = \left[-\tilde{p} + 2\delta^2 \frac{\partial}{\partial z} u_3 \right]_\Gamma, \quad (6c)$$

where

$$\mathbf{u}|_\Gamma = (0, 0, i\epsilon\omega_0 \zeta), \quad (7a)$$

$$\mathbf{u}|_{\Gamma_w} = \left(\frac{i\omega_0 \zeta_w}{\epsilon}, 0, 0 \right), \quad (7b)$$

$$\mathbf{u}|_{\Gamma_R} = \left(-\frac{i\omega_0 \zeta_w}{\epsilon}, 0, 0 \right). \quad (7c)$$

In the last two boundary conditions, it is assumed that the displacement of the upper, and lower, window has the form

$$\eta_w = \zeta_w(y, z) e^{i\omega t}.$$

Also, in addition to (7), \mathbf{u} satisfies the no-slip condition on the remainder of the cochlear wall and bony shelf, and ζ satisfies the simply supported boundary conditions described earlier.

As a consequence of the symmetry of the above problem, \tilde{p} , u_1 and u_2 are odd functions of z , whereas u_3 is an even function. Therefore, it suffices to consider only the motion in the scala vestibuli; that is, in the upper chamber. In this case, the stress on the basilar membrane in (6c) due to the fluid is simply twice the value obtained from the scala vestibuli.

It should be pointed out that (4) is not used simply to incorporate a higher-frequency regime into the asymptotics. The particular dependence used here corresponds to a distinguished limit, which is appropriate in problems involving several parameters (see, for example O'Malley 1967). There are, of course, other distinguished limits that can, and probably should, be studied. However, in what follows, the dependence given in (4) is used.

4. Asymptotic expansions

To solve (6) and (7), we now introduce asymptotic expansions based on small ϵ . As is apparent from (6a), this will necessitate a study of viscous boundary layers as well as an edge layer near the upper window. A summary of the results of the analysis to follow can be found in §5.

Inviscid region

As mentioned above, away from the immediate vicinity of the stapes, the fluid flow is composed of an inviscid core and a boundary-layer region very near the cochlear wall. In the inviscid region, the appropriate expansions are

$$u_1 \sim \frac{1}{\epsilon} \exp\left(\frac{\theta}{\epsilon} + \frac{\phi}{\epsilon^{\frac{1}{2}}}\right) [u_{10}(x, y, z) + \epsilon^{\frac{1}{2}}u_{11} + \dots], \quad (8a)$$

$$u_2 \sim \exp\left(\frac{\theta}{\epsilon} + \frac{\phi}{\epsilon^{\frac{1}{2}}}\right) [u_{20}(x, y, z) + \epsilon^{\frac{1}{2}}u_{21} + \dots], \quad (8b)$$

$$u_3 \sim \exp\left(\frac{\theta}{\epsilon} + \frac{\phi}{\epsilon^{\frac{1}{2}}}\right) [u_{30}(x, y, z) + \epsilon^{\frac{1}{2}}u_{31} + \dots], \quad (8c)$$

$$\tilde{p} \sim \frac{1}{\epsilon} \exp\left(\frac{\theta}{\epsilon} + \frac{\phi}{\epsilon^{\frac{1}{2}}}\right) [p_0(x, y, z) + \epsilon^{\frac{1}{2}}p_1 + \dots], \quad (8d)$$

where θ and ϕ depend only on x .

Inserting (8) into (6), one finds that

$$i\omega_0 u_{10} = -\theta_x p_0, \quad i\omega_0 u_{20} = -\frac{\partial}{\partial y} p_0, \quad i\omega_0 u_{30} = -\frac{\partial}{\partial z} p_0, \quad (9a, b, c)$$

$$\theta_x u_{10} + \frac{\partial}{\partial y} u_{20} + \frac{\partial}{\partial z} u_{30} = 0. \quad (9d)$$

From this, it follows that

$$\left(\frac{\partial^2}{\partial y^2} + \frac{\partial^2}{\partial z^2}\right) p_0 + \theta_x^2 p_0 = 0. \quad (10)$$

The boundary conditions for p_0 are determined later by matching the above functions with the boundary-layer solution. In the meantime, note that (10) is to be solved in the cross-sectional region Ψ , and so, as it stands, the x -dependence of p_0 is not completely determined.

To find the function $\phi(x)$, we need to consider the problem for the $O(\epsilon^{\frac{1}{2}})$ terms in (8). From (6), one finds that this is

$$i\omega_0 u_{11} = -\phi_x p_0 - \theta_x p_1, \quad i\omega_0 u_{21} = -\frac{\partial}{\partial y} p_1, \quad i\omega_0 u_{31} = -\frac{\partial}{\partial z} p_1, \quad (11a, b, c)$$

$$\theta_x u_{11} + \phi_x u_{10} + \frac{\partial}{\partial y} u_{21} + \frac{\partial}{\partial z} u_{31} = 0. \quad (11d)$$

From this, it follows that

$$\left(\frac{\partial^2}{\partial y^2} + \frac{\partial^2}{\partial z^2}\right) p_1 + \theta_x^2 p_1 = -2\theta_x \phi_x p_0. \quad (12)$$

Again this is to be solved in Ψ . Once the boundary conditions for p_1 are determined, (12) is used to find $\phi(x)$ by multiplying this equation by p_0 and then integrating over

the cross-section. However, note that (11) or (12) do not resolve the indeterminacy of p_0 as a function of x . To do this, it is necessary to consider the problem for the $O(\epsilon)$ terms in (8). Carrying out the details, one finds that, for p_2 , the analogue of (12) is

$$\left(\frac{\partial^2}{\partial y^2} + \frac{\partial^2}{\partial z^2}\right) p_2 + \theta_x^2 p_2 = -2\theta_x \phi_x p_1 - (\phi_x^2 + \theta_{xx}) p_0 - 2\theta_x \frac{\partial}{\partial x} p_0. \quad (13)$$

Boundary-layer region

It still remains to find the appropriate boundary conditions for p_0 , p_1 and p_2 as well as to find the reduced equation for the motion of the basilar membrane. For the boundary layer above the basilar membrane, we introduce the co-ordinate $\tilde{z} = z\epsilon^{-\frac{1}{2}}$. In this case, the problem takes the form

$$i\omega_0 \mathbf{u} - \delta^2 \left(\epsilon^2 \frac{\partial^2}{\partial x^2} + \epsilon \frac{\partial^2}{\partial y^2} + \frac{\partial^2}{\partial \tilde{z}^2} \right) \mathbf{u} = - \left(\epsilon \frac{\partial}{\partial x}, \epsilon \frac{\partial}{\partial y}, \epsilon^{\frac{1}{2}} \frac{\partial}{\partial \tilde{z}} \right) \tilde{p}, \quad (14a)$$

$$\epsilon^{\frac{1}{2}} \frac{\partial}{\partial x} u_1 + \epsilon^{\frac{1}{2}} \frac{\partial}{\partial y} u_2 + \frac{\partial}{\partial \tilde{z}} u_3 = 0, \quad (14b)$$

$$\left(\frac{\partial^4}{\partial y^4} + 2\epsilon^2 D_3 \frac{\partial^4}{\partial x^2 \partial y^2} + \epsilon^4 D_1 \frac{\partial^4}{\partial x^4} - \frac{\omega_0^2}{\alpha_0} \epsilon^2 \right) \zeta = \left[-\tilde{p} + 2\delta^2 \frac{1}{\epsilon^{\frac{1}{2}}} \frac{\partial}{\partial \tilde{z}} v_3 \right]_{\Gamma}. \quad (14c)$$

The expansions have essentially the same form as in the inviscid region, and so

$$u_1 \sim \frac{1}{\epsilon} \exp\left(\frac{\theta}{\epsilon} + \frac{\phi}{\epsilon^{\frac{1}{2}}}\right) [U_{10}(x, y, \tilde{z}) + \epsilon^{\frac{1}{2}} U_{11} + \dots], \quad (15a)$$

$$u_2 \sim \exp\left(\frac{\theta}{\epsilon} + \frac{\phi}{\epsilon^{\frac{1}{2}}}\right) [U_{20}(x, y, \tilde{z}) + \epsilon^{\frac{1}{2}} U_{21} + \dots], \quad (15b)$$

$$u_3 \sim \exp\left(\frac{\theta}{\epsilon} + \frac{\phi}{\epsilon^{\frac{1}{2}}}\right) [U_{30}(x, y, \tilde{z}) + \epsilon^{\frac{1}{2}} U_{31} + \dots], \quad (15c)$$

$$\tilde{p} \sim \frac{1}{\epsilon} \exp\left(\frac{\theta}{\epsilon} + \frac{\phi}{\epsilon^{\frac{1}{2}}}\right) [P_0(x, y, \tilde{z}) + \epsilon^{\frac{1}{2}} P_1 + \dots], \quad (15d)$$

$$\zeta \sim \frac{1}{\epsilon} \exp\left(\frac{\theta}{\epsilon} + \frac{\phi}{\epsilon^{\frac{1}{2}}}\right) [\zeta_0(x, y) + \epsilon^{\frac{1}{2}} \zeta_1 + \dots]. \quad (15e)$$

Introducing these expansions into (14), and matching the solutions with those from the inviscid region, one finds, not unexpectedly, that

$$u_{30}|_{\Gamma} = U_{30} = i\omega_0 \zeta_0(x, y), \quad P_0 = p_0|_{\Gamma}.$$

With this, it follows that

$$\left(\frac{\partial^4}{\partial y^4} + 2D_3 \theta_x^2 \frac{\partial^2}{\partial y^2} + D_1 \theta_x^4 \right) \zeta_0 = -[p_0]_{\Gamma}, \quad (16)$$

$$\frac{\partial}{\partial \tilde{z}} p_0 \Big|_{\Gamma} = \omega_0^2 \zeta_0. \quad (17)$$

Similarly, on the rigid portion Σ of the cross-sectional boundary we have that

$$\frac{\partial}{\partial n} p_0 \Big|_{\Sigma} = 0, \quad (18)$$

where n refers to the unit outward normal to Σ .

Note that, from (16), the normal stress on the basilar membrane due to the vertical

component of the fluid velocity does not contribute to the first term. In fact, from (14) one can see that it does not enter until the $O(\epsilon)$ problem.

To determine the boundary conditions for p_1 and p_2 it is necessary to consider the next two higher-order problems in the boundary layer. The details of the calculations are not given here. In essence, as in the first-order problem, the boundary condition to be used in the inviscid problem comes from the vertical, or normal, component of the velocity. In particular, one finds that on the basilar membrane

$$u_{31}|_{\Gamma} = i\omega_0 \zeta_1(x, y) - \frac{i\beta}{\omega_0} \frac{\partial^2}{\partial z^2} p_0 \Big|_{\Gamma}, \quad (19)$$

$$u_{32}|_{\Gamma} = i\omega_0 \zeta_2(x, y) - \frac{i}{\omega_0} \left(\beta \frac{\partial^2}{\partial z^2} p_1 + \beta^2 \frac{\partial^3}{\partial z^3} p_0 \right) \Big|_{\Gamma}, \quad (20)$$

where

$$\beta^2 = \frac{\delta^2}{i\omega_0}.$$

Also, on the rigid portion of the cochlear wall

$$u_{31}|_{\Sigma} = -\frac{i\beta}{\omega_0} \frac{\partial^2}{\partial n^2} p_0 \Big|_{\Sigma}, \quad (21)$$

$$u_{32}|_{\Sigma} = -\frac{i}{\omega_0} \left(\beta \frac{\partial^2}{\partial n^2} p_1 + \beta^2 \frac{\partial^2}{\partial n^2} p_0 \right) \Big|_{\Sigma}. \quad (22)$$

The $O(\epsilon^{\frac{1}{2}})$ problem for the displacement of the basilar membrane is

$$\left(\frac{\partial^4}{\partial y^4} + 2D_3 \theta_x^2 \frac{\partial^2}{\partial y^2} + D_1 \theta_x^4 \right) \zeta_1 + 4\theta_x \phi_x \left(D_3 \frac{\partial^2}{\partial y^2} + D_1 \theta_x^2 \right) \zeta_0 = -[p_1]_{\Gamma}. \quad (23)$$

Now, with (19) and (21) the boundary conditions for p_1 are

$$\frac{\partial}{\partial z} p_1 \Big|_{\Gamma} = \omega_0^2 \zeta_1 - \beta \frac{\partial^2}{\partial z^2} p_0 \Big|_{\Gamma}. \quad (24a)$$

$$\frac{\partial}{\partial n} p_1 \Big|_{\Sigma} = \beta \frac{\partial^2}{\partial n^2} p_0 \Big|_{\Sigma}. \quad (24b)$$

The function $\phi(x)$ can now be determined, aside from an integration constant, by multiplying (12) by p_0 , using Green's theorem, and then introducing (23) and (24). The result is given in (33).

As with p_0 , p_1 is not entirely determined by (12) and (24). In particular, any multiple of the function p_0 can be added to p_1 . The same holds for p_2 . This can be resolved, as it is for p_0 , through the use of consistency conditions from the higher-order problems. However, as this indeterminacy has no effect on what follows, it will be ignored.

In any case, it still remains to resolve the dependence of p_0 on the longitudinal coordinate. This comes by setting

$$p_0(x, y, z) = A_r(x) p_r(x, y, z),$$

where p_r is a particular solution of (10). Multiplying (13) by p_0 , integrating over the cross-section, and then using Green's theorem, one finds that

$$\frac{d}{dx} A_r^2(x) + f(x) A_r^2(x) = 0, \quad (25a)$$

where

$$f(x) = \frac{d}{dx} \ln \left(\theta_x \int_{\Psi} p_r^2 \right) + O(\beta^2). \quad (25b)$$

Therefore, ignoring the $O(\beta^2)$ terms in (25b), we have

$$A_r^2(x) = \frac{A_0^2}{\theta_x \int_{\mathbb{V}} p_r^2}. \quad (26)$$

Edge layer

To complete the problem, it is necessary to take into account both an edge layer, as well as a viscous boundary layer, near the oval window. The reason is that this will determine the correct boundary conditions to be used at the basal end.

The co-ordinate for the viscous boundary layer is $\tilde{x} = x\epsilon^{-\frac{3}{2}}$, and for the edge layer it is $\hat{x} = x\epsilon^{-1}$. Without going through the details, it is found that the matching condition comes from the conservation of the fluid volume. Thus, it is required that

$$i\omega_0 \int_{\Gamma_w} \zeta_w dy dz = \int_{\mathbb{V}} u_{10} dy dz \quad \text{for } x = 0, \quad (27)$$

where

$$\theta(0) = \phi(0) = 0. \quad (28)$$

Therefore

$$\theta_x \int_{\mathbb{V}} p_0 dy dz = \omega_0^2 \int_{\Gamma_w} \zeta_w dy dz \quad \text{for } x = 0. \quad (29)$$

For the special case of a uniform unit displacement of the stapes, (29) reduces to

$$\theta_x \int_{\mathbb{V}} p_0 dy dz = \omega_0^2 A_w \quad \text{for } x = 0, \quad (30)$$

where A_w represents the (dimensionless) area of the oval window.

As a final remark, it should be pointed out that (27) omits the displacement of the basilar membrane in the edge layer. This has no effect on the analysis to follow. The reason is that this boundary condition is actually only used when discussing tuning curves, and so it is only necessary to know the correct dependence on ω_0 . Consequently, (30) is sufficient.

5. Summary of the reduction

To summarize the results of §4, it is found that the solution of (6) and (7) is, approximately,

$$\hat{p} \sim \frac{1}{\epsilon} e^{\psi(x)} p_0(x, y, z), \quad (31a)$$

$$\zeta \sim \frac{1}{\epsilon} e^{\psi(x)} \zeta_0(x, y, z), \quad (31b)$$

$$u_1 \sim \frac{1}{\epsilon} e^{\psi(x)} \frac{i\theta_x}{\omega_0} p_0(x, y, z), \quad (31c)$$

$$u_2 \sim e^{\psi(x)} \frac{i}{\omega_0} \frac{\partial}{\partial y} p_0(x, y, z), \quad (31d)$$

$$u_3 \sim e^{\psi(x)} \frac{i}{\omega_0} \frac{\partial}{\partial z} p_0(x, y, z), \quad (31e)$$

where

$$\psi(x) = \frac{1}{\epsilon} \theta(x) + \frac{1}{\epsilon^{\frac{1}{2}}} \phi(x).$$

The functions $\theta(x)$, p_0 and ζ_0 are solutions of

$$\left(\frac{\partial^2}{\partial y^2} + \frac{\partial^2}{\partial z^2}\right)p_0 + \theta_x^2 p_0 = 0 \quad \text{in } \Psi, \quad (32a)$$

$$\left(\frac{\partial^4}{\partial y^4} + 2\theta_x^2 D_3 \frac{\partial^2}{\partial y^2} + D_1 \theta_x^4\right)\zeta_0 = -2p_0(x, y, 0) \quad \text{in } \Gamma, \quad (32b)$$

where

$$\frac{\partial}{\partial z} p_0 = \omega_0^2 \zeta_0 \quad \text{on } \Gamma, \quad (32c)$$

$$\frac{\partial}{\partial n} p_0 = 0 \quad \text{on } \Sigma, \quad (32d)$$

$$\zeta_0 = \frac{\partial^2}{\partial y^2} \zeta_0 = 0 \quad \text{for } y = G_{\pm}(x). \quad (32e)$$

The function $\phi(x)$ is specified later (equation (33)).

Therefore $\theta(x)$ can be thought of as an eigenvalue, and p_0 and ζ_0 as the corresponding eigenfunctions, of (32). However, note that (32) only determines how p_0 and ζ_0 depend on y and z , since these functions can be multiplied by an arbitrary function of x and still satisfy (32). This is not true for θ . Also, the above approximations for u_1 and u_2 do not hold in the immediate vicinity of the cochlear boundary because of the influence of the viscous boundary layer in this region. An eigenvalue problem similar to (32a) has also been obtained by Chadwick (1981), although his treatment of the viscosity and his asymptotic approximations are different from those used here. In doing so, he illustrates some of the interesting effects the inertia of the basilar membrane can have on the dynamic response.

In the examples to be discussed later, the function $\theta(x)$ is imaginary. Consequently, we will refer to it as the phase function, although, as it turns out, $\phi(x)$ also contributes slightly to the overall phase. As in the low-frequency theory, the phase function is determined from the inviscid problem. However, it should be emphasized that the travelling-wave solution that comes from (31) is due entirely to the viscosity. In particular, it is implicitly assumed here that the viscous attenuation of the wave is such that the boundary conditions at the apical end can be ignored. Even with a non-zero viscosity, this imposes a lower bound on the frequencies for which the above analysis is applicable. As we shall see, for the human cochlea this limit is somewhere between 500 and 1000 Hz. If the fluid is inviscid, so that there is no damping in the system, then only standing waves are obtained because of the finite geometry. Finally, note that, unlike the low-frequency theory, the fluid flow is fully three-dimensional and that the longitudinal coupling in the basilar membrane is present in the reduced problem.

The function $\phi(x)$ is found from the consistency condition for the $O(\epsilon^{\frac{1}{2}})$ terms in the above expansions. In particular, it is found that

$$\phi_x(x) = -\frac{\beta}{2\theta_x} \int_{\partial\Psi} p_0 \frac{\partial^2}{\partial n^2} p_0 / \left\{ \int_{\Psi} p_0^2 + \omega_0^2 \int_{\Gamma_x} \left[D_3 \left(\frac{\partial}{\partial y} \zeta_0 \right)^2 - D_1 \theta_x^2 \zeta_0^2 \right] dy \right\}, \quad (33)$$

where $\beta = \delta(i\omega_0)^{-\frac{1}{2}}$. Assuming, for the moment, that the phase function is imaginary, it follows that the integrals in (33) are positive. Therefore $\phi(x)$ is complex-valued, and so it is the principal contributor to the attenuation of the wave. With this in mind

note, from (33), that the bending and twisting rigidities D_1 and D_3 act to reduce the damping. In other words, the longitudinal coupling in the basilar membrane acts to reduce the damping, which is consistent with the observations of Steele & Taber (1979).

To complete the solution, the dependence of p_0 and ζ_0 on x has to be determined. This comes from the problem for the $O(\epsilon)$ terms in the expansions. Letting

$$p_0 = A_r(x) p_r(x, y, z), \quad \zeta_0 = A_r(x) \zeta_r(x, y),$$

where p_r and ζ_r form a particular solution of (32), then from (26)

$$A_r^2(x) = \frac{A_0^2}{\theta_x \int_{\Psi} p_r^2}. \quad (34)$$

The constant A_0 is determined from the boundary condition at the basal end. From (30) one finds that

$$A_0 = \frac{\omega_0^2 A_w}{\int_{\Psi} p_r} \left(\frac{\int_{\Psi} p_r^2}{\theta_x} \right)^{\frac{1}{2}} \quad \text{for } x = 0, \quad (35)$$

$$\theta(0) = \phi(0) = 0. \quad (36)$$

The eigenvalue problem (32), along with (33)–(36), determines the complete solution to the first-order approximation. It applies to any cross-sectional geometry so long as the symmetry conditions stated in §2 are satisfied. As for $\theta(x)$, there is some question as to how many eigenvalues there are for (32). In the example to be discussed next there is, in fact, only one. More precisely, there is only one value for θ_x^2 , which in turn results in two values for θ . The correction to $\theta(x)$, i.e. $\phi(x)$, is, as has already been pointed out, principally responsible for the attenuation of the wave. With this in mind, note that it depends on the entire cross-section and not just on the portion above the basilar membrane. This is consistent with what is found in the low-frequency theory. It also shows that it is not sufficient to consider only the boundary layer above the basilar membrane.

6. Solution of eigenvalue problem

There are a number of ways to solve the eigenvalue problem for the phase function. The one to be used here involves the use of the Green function $\mathcal{G}(x, y, z; \xi, \tau)$, which is the solution of

$$\left(\frac{\partial^2}{\partial \xi^2} + \frac{\partial^2}{\partial \tau^2} \right) \mathcal{G} + \theta_x^2 \mathcal{G} = \delta(\xi - y) \delta(\tau - z) \quad \text{in } \Psi,$$

where

$$\mathbf{n} \cdot (\mathcal{G}_\xi, \mathcal{G}_\tau) = 0 \quad \text{on } \partial\Psi,$$

and $\delta(\)$ is Dirac's delta function. It is being assumed, for the moment, that θ_x^2 is known. Also, the boundary condition means that the normal derivative of \mathcal{G} , with respect to the (ξ, τ) -co-ordinates, is zero. With this, the solution of (32a, c, d) is

$$p_0(x, y, z) = \omega_0^2 \int_{\Gamma_r} \zeta_0(x, \xi) \mathcal{G}(x, y, z; \xi, 0) d\xi. \quad (37)$$

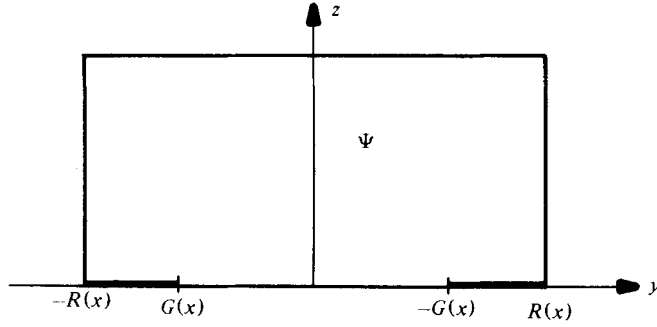


FIGURE 2. Transverse cross-section of the cochlea used in solving eigenvalue problem.

The eigenvalue problem now takes the form

$$\left(\frac{\partial^4}{\partial y^4} + 2\theta_x^2 D_3 \frac{\partial^2}{\partial y^2} + \theta_x^4 D_1\right) \zeta_0 = -2\omega_0^2 \int_{\Gamma_x} \zeta_0(x, \xi) \mathcal{K}(x, y; \xi) d\xi, \quad (38)$$

where

$$\mathcal{K}(x, y; \xi) = \mathcal{G}(x, y, 0; \xi, 0).$$

To continue, it is necessary to specify the geometry, and so it is now assumed that the upper and lower cross-sections are rectangular (figure 2). At the same time, the basilar membrane is located in the centre of the cross-section with $G(x) = G_+(x) = -G_-(x)$. However, both G and R are still arbitrary functions of x . Another assumption that is made, to facilitate the discussion, is that $D_1 = D_3 = 0$. More precisely, it is assumed that, except in the y -direction, the bending and twisting rigidities of the basilar membrane are so weak that they do not contribute until the $O(\epsilon^{\frac{3}{2}})$ problem. This assumption is consistent with the observations of Voldrich (1978).

As a consequence of the symmetry of the geometry in the y -co-ordinate, and assuming the driving function ζ_w satisfies the same symmetry condition, both the pressure $\hat{p}(x, y, z)$ and the displacement of the basilar membrane $\zeta(x, y)$ are even functions of y . This observation helps to simplify the Fourier expansions introduced below. Also, note that with the assumption on the bending and twisting rigidities it is relatively easy to show that the function θ_x^2 is real. This can be done by multiplying (32) by \bar{p}_0 and integrating over the cross-section, from which one finds that

$$\theta_x^2 \int_{\Psi} |p_0|^2 = \int_{\Psi} |\nabla_{y,z} p_0|^2 - \frac{1}{2}\omega_0^2 \int_{\Gamma_x} \left| \frac{\partial^2}{\partial y^2} \zeta_0 \right|^2, \quad (39)$$

where Γ_x refers to the portion of the basilar membrane in the cross-section located at x .

With the assumption of a rectangular geometry, it is possible to find the Green function explicitly. It is given as

$$\mathcal{G}(x, y, z; \xi, \tau) = -2 \sum_{\substack{n, m=0 \\ m \text{ even}}}^{\infty} c_n c_m \frac{\cos \alpha_n z \cos \alpha_n \tau \cos \gamma_m (y + R) \cos \gamma_m (\xi + R)}{(\pi/2R)^2 (4n^2 + m^2) - \theta_x^2},$$

where

$$c_m = \begin{cases} \frac{1}{2R} & \text{if } m = 0, \\ \frac{1}{R} & \text{if } m \neq 0, \end{cases}$$

$$\alpha_n = n\pi/R, \quad \gamma_m = m\pi/2R.$$

Therefore, from (37)

$$p_0 = - \sum_{m=0}^{\infty} c_{2m} \cos \gamma_{2m}(y+R) \frac{\cosh k_{2m}(R-z)}{k_{2m} \sinh Rk_{2m}} \omega_0^2 \int_{-G}^G \zeta_0 \cos \gamma_{2m}(\xi+R) d\xi, \quad (40)$$

where
$$k_{2m}^2 = \left(\frac{\pi}{2R}\right)^2 m^2 - \theta_x^2.$$

To obtain (40) from (37), the following identity is used (Hansen 1975):

$$2 \sum_{n=0}^{\infty} c_n \frac{\cos \alpha_n z}{\left(\frac{\pi}{2R}\right)^2 (4n^2 + m^2) - \theta_x^2} = \frac{\cosh k_m(R-z)}{k_m \sinh Rk_m}.$$

With (40), the integro-differential equation (38) becomes

$$\frac{\partial^4}{\partial y^4} \zeta_0 = 2 \sum_{m=0}^{\infty} c_m \cos \gamma_{2m}(y+R) \frac{\coth Rk_{2m}}{k_{2m}} \omega_0^2 \int_{-G}^G \zeta_0 \cos \gamma_{2m}(\xi+R) d\xi. \quad (41)$$

The right-hand side of (41) is a separable function, and so, with (32e), it follows that

$$\zeta_0(x, y) = a_0(y^4 - 6G^2y^2 + 5G^4) + \sum_{m=1}^{\infty} a_{2m} \left[\frac{1}{\gamma_{2m}^4} \cos \gamma_{2m}(y+R) + B_{2m}y^2 + D_{2m} \right], \quad (42)$$

where

$$B_{2m} = \frac{(-1)^m \cos \gamma_{2m} G}{2\gamma_{2m}^2},$$

$$D_{2m} = \frac{(-1)^{m+1}(1 + \gamma_{2m}^2 G^2) \cos \gamma_{2m} G}{2\gamma_{2m}^4}.$$

Note that both B_{2m} and D_{2m} are functions of x . The coefficients $a_i(x)$ are determined by substituting (42) into (41), from which one finds that

$$a_0 = \lambda_0 \omega_0^2 \int_{-G}^G \zeta_0 d\xi, \quad (43a)$$

and, for $m \neq 0$,

$$a_{2m} = \lambda_{2m} \omega_0^2 \int_{-G}^G \zeta_0 \cos \gamma_{2m}(\xi+R) d\xi, \quad (43b)$$

where
$$\lambda_0 = \frac{\coth Rk_0}{24Rk_0}, \quad \lambda_{2m} = \frac{2 \coth Rk_{2m}}{Rk_{2m}}. \quad (44a, b)$$

Therefore, from (42) it follows that

$$a_{2m} = \lambda_{2m} \omega_0^2 \sum_{n=0}^{\infty} \alpha_{m,n} a_{2n}, \quad (45)$$

where $\alpha_{m,n}$ represents the values of the respective integrals one obtains in substituting (42) into (43). This can be written in matrix form as

$$\mathbf{a} = \mathbf{M}\mathbf{a}, \quad (46)$$

where \mathbf{M} represents the matrix of coefficients obtained from the sums in (45), and

$$\mathbf{a} = \begin{pmatrix} a_0 \\ a_2 \\ \vdots \end{pmatrix}.$$

Consequently, the original eigenvalue problem has been reduced to an algebraic problem, although there is an infinite number of unknowns. However, it is only necessary to use the first two or three terms to obtain a reasonably accurate approximation to the solution. As a final comment, note that, by using a first-term approximation in (42), one obtains a computational procedure similar to that used by Steele & Taber (1979).

Once the a_i and the phase function are determined from (46), one can calculate $\phi(x)$ from (33) and $A_r(x)$ from (34). Also, from (40) and (43),

$$p_0 = - \sum_{m=0}^{\infty} \hat{c}_m a_{2m} \frac{\cosh k_{2m}(R-z)}{\cosh Rk_{2m}} \cos \gamma_{2m}(y+R), \quad (47)$$

where

$$\hat{c}_m = \begin{cases} \frac{1}{2} & \text{if } m \neq 0, \\ 12 & \text{if } m = 0. \end{cases}$$

7. Numerical example

To apply the results of the following sections to the cochlea, we now let $B = 0.05$ cm, $L = 3.5$ cm, $\nu = 0.008$ cm s⁻¹, $\rho = 1.0$ g cm⁻³ and

$$D_2^* = \frac{Eh^3}{12(1-\sigma^2)},$$

where $E = 4 \times 10^6$ dyn cm⁻², $h = 4 \times 10^{-3}$ cm and $\sigma = 0.3$. Also,

$$G(x) = \frac{1}{12}(5x+1), \quad R^* = 0.08 \text{ cm}. \quad (48), (49)$$

The above value for R^* gives a constant cross-sectional area of 0.01 cm². These values are representative of those found in the human cochlea and are the same as used for the low-frequency theory (Holmes 1981).

As mentioned earlier, it is only necessary to use the first three terms in (42) to obtain a reasonably accurate approximation. In this case, (46) takes the form

$$\mathbf{M} \begin{pmatrix} a_0 \\ a_2 \\ a_4 \end{pmatrix} = \begin{pmatrix} a_0 \\ a_2 \\ a_4 \end{pmatrix}. \quad (50)$$

Consequently, θ_x^2 is a solution of the equation

$$\det(\mathbf{M} - \mathbf{I}) = 0, \quad (51)$$

where \mathbf{I} represents the 3×3 identity matrix. Solving (51), one finds that $\theta_x = \pm ik(x)$, where $k(x)$ is a positive function of x . As we want waves that travel in the direction of increasing x then, using (36),

$$\theta(x) = -i \int_0^x k(s) ds. \quad (52)$$

With this, it is a simple matter to solve (50) for a_2 and a_4 in terms of a_0 , and then to calculate $\phi(x)$ and $A_r(x)$ from (33) and (34).

The roots of (51) are found using the secant method, where the initial approximations are based on the value obtained from the low-frequency theory. At each x -location it takes, on the average, four iterations to obtain the root with a relative error of less than 10^{-3} . After determining the phase function, $\phi(x)$ is found from (33),

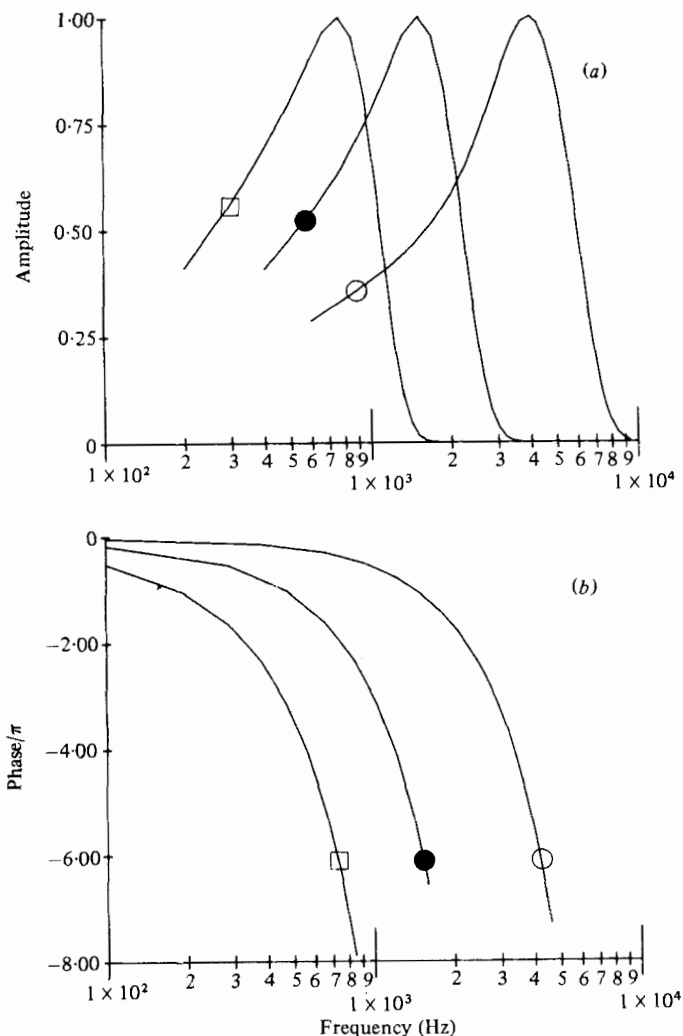


FIGURE 3. Normalized amplitude (a) and phase (b) of the wave on the basilar membrane, as functions of frequency, for $x = 0.25$ (\square); 0.5 (\bullet); 0.75 (\circ).

using Simpson's rule to evaluate the integrals. In the process, forty points are used along the x -axis. These methods are easy to implement and fairly fast. For example, on an IBM 3033, the tuning and phase curves shown in figure 3, in total take less than 2 s in CPU time to compute. Therefore, the method is comparable in terms of computing time with Steele & Taber (1979).

The results of the calculations are shown in figures 3–5. In the first, figure 3, the tuning and phase curves are shown for the points $x = \frac{1}{4}$, $\frac{1}{2}$ and $\frac{3}{4}$. The tuning curve represents the ratio of the amplitude of the basilar membrane to the amplitude of the stapes. So the curves shown in the figure represent the amplitude obtained from (42), with $y = 0$, and with $\zeta_w = 1$ in (29). In conjunction with this, the amplitude, or envelope, of the centre-line deflection of the basilar membrane is shown in figure 4 for the driving frequencies that produced the maximum amplitude in figure 3. Finally,

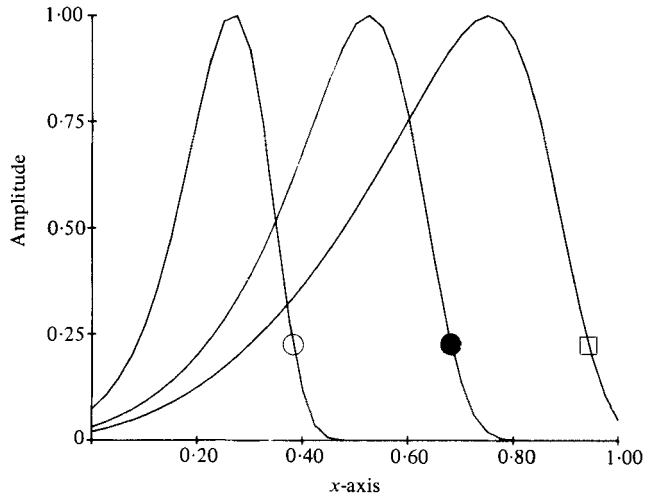


FIGURE 4. Normalized amplitude of the wave on the basilar membrane, as a function of position, for driving frequencies corresponding to 760 Hz (\square), 1500 Hz (\bullet), 4000 Hz (\circ).

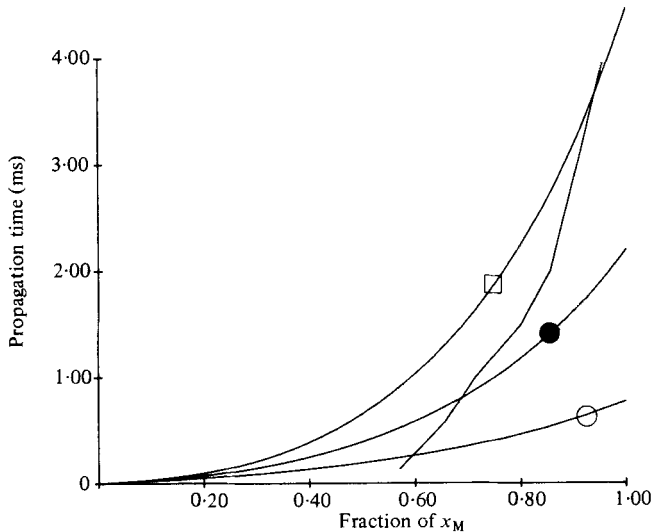


FIGURE 5. Time it takes the wave to reach the point of maximum response x_M for frequencies used in figure 4. Also shown, by the unmarked curve, are the values obtained by von Békésy (1960) (for which $x_M = 1$).

the time it takes the wave to propagate from the basal end to the longitudinal location of the maximum response, which is denoted by x_M , is shown in figure 5.

The curves in figure 3 show a reasonably sharp tuning, much more so than is obtained from the low-frequency theory. Nevertheless, they are not as sharp as might be expected from neural measurements. They are, in a qualitative sense, in agreement with Rhode's (1971) measurements, although they do not show a constant phase angle for high frequencies. Also, the propagation times shown in figure 5 are in agreement with von Békésy's (1960) observations.

In figure 4 it can be seen that the amplitude is not negligible at the apical end for

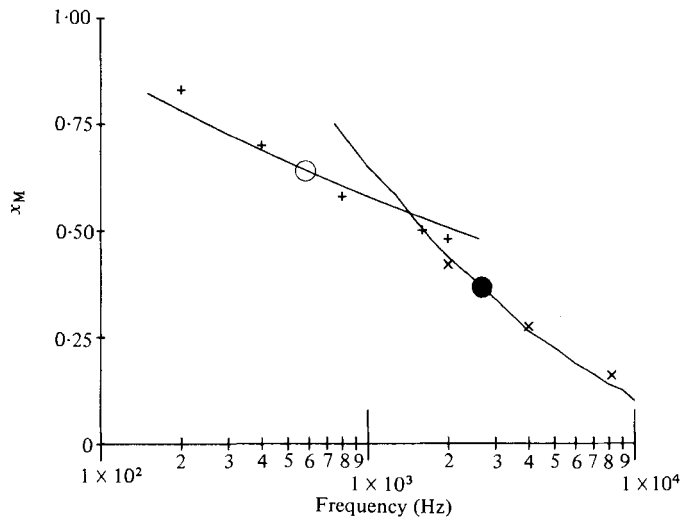


FIGURE 6. The dependence of the point of maximum response on frequency. Shown are the curves obtained from the low-frequency theory (○) and the present model (●); as well as the experimental results of von Békésy (1960) (+) and Crowe *et al.* (1934) (x).

the 760 Hz curve. Consequently, the results of this theory begin to become questionable for frequencies any less than this. Although the analysis can be corrected, to some extent, by re-applying it to the reflected wave, it is easier to use the low-frequency theory in this region.

The point of maximum response on the basilar membrane for the curves in figure 4 agree with empirical measurements. In fact, if one plots the dependence of the longitudinal location of the maximum response, as a function of the frequency, the curve shown in figure 6 is obtained. The measurements of von Békésy (1960) and Crowe, Guild & Polvogt (1934) are also shown, as well as the location of x_M as determined from the low-frequency theory. For the low-frequency curve, the values given earlier are used, except for the thickness which is taken to be 1.3×10^{-3} cm. This figure indicates the frequency regimes in which the two theories are valid. For example, the upper limit of the low-frequency theory seems to be in the neighbourhood of 2000 Hz. The lower limit of the present theory is around 1000 Hz, which is consistent with the comments of the preceding paragraph. All in all, in their respective regions, these theories agree quite well with the experimental results. Also, note that the lower limit for the present theory can be extended somewhat by taking into account the decreasing thickness of the basilar membrane. In doing this, it would not be necessary to use two different values for the thickness when comparing it with the low-frequency theory.

Comparing figures 3 and 5, one can see that the tuning and amplitude curves agree as to the frequency and spatial location of the maximum response. For example, the frequency producing the maximum response at $x = 0.25$ is approximately 4000 Hz, and, equivalently, the point of maximum response for a driving frequency of 4000 Hz is $x = 0.25$. This does not happen with the low-frequency theory.

Another difference between the two theories is the dependence of the wave velocity on the frequency. In the present theory, the wave slows down with increasing frequency (figure 6). In other words, the velocity of the wave is a monotonically de-

creasing function of the frequency. This dependence, although contrary to von Békésy's observations, is consistent with the measurements of Robles, Rhode & Geisler (1976).

As illustrated in the last few paragraphs, the present model is quite capable of describing most of the high-frequency behaviour in the cochlea. In doing this, it has been seen that, not unexpectedly, there are differences with some of the results from the low-frequency theory. However, it is interesting to note that the low-frequency theory can be obtained, in a sense, from the results of the present analysis. In particular, if one assumes that p_0 and ζ_0 have the form as in the low-frequency theory, which means that $a_1 = a_2 = \dots = 0$ in (42) and (47), then one obtains the low-frequency WKB phase, attenuation and amplitude functions from (39), (33) and (34), respectively (Chadwick & Cole 1979).

The model used here can be generalized in a number of ways without greatly affecting the analysis used in finding the solution. For example, if one were to model the basilar membrane as an anisotropic plate with a varying thickness, then the only change would be to the left-hand side of (32*b*). In this case, the D_2^* used in the non-dimensionalization would be a typical value of the rigidity in the y -direction (Holmes 1981). Through the use of the correspondence principle, one could also assume that the plate is viscoelastic. However, this would mean that the bending rigidities depend on the frequency. In this case, because of (4), the analysis could be affected. It is expected, though, that with something like the standard linear model the analysis extends in a straightforward manner.

REFERENCES

- ALLEN, J. B. 1977 Two-dimensional cochlear fluid model: new results. *J. Acoust. Soc. Am.* **61**, 110–119.
- VON BÉKÉSY, G. 1960 *Experiments in Hearing*. McGraw-Hill.
- DE BOER, E. 1979 Short-wave world revisited: resonance in a two-dimensional cochlear model. *Hearing Res.* **1**, 253–281.
- CHADWICK, R. 1981 Studies in cochlear mechanics. In *Math. Modeling of the Hearing Process* (ed. M. Holmes & L. Rubinfeld), Lecture Notes in Biomathematics, Vol. **43**, pp. 9–54. Springer.
- CHADWICK, R. & COLE, J. 1979 Modes and waves in the cochlea. *Mech. Res. Comm.* **6**, 177–184.
- CROWE, S., GUILD, S. & POLVOGT, L. 1934 Observations on the pathology of high-tone deafness. *Bull. Johns Hopkins Hosp.* **54**, 315–379.
- HANSEN, E. R. 1975 *A Table of Series and Products*. Prentice-Hall.
- HOLMES, M. H. 1981 A study of the transient problem in the cochlea. *J. Acoust. Soc. Am.* **69**, 751–759.
- LESSER, M. B. & BERKLEY, D. A. 1972 Fluid mechanics of the cochlea. *J. Fluid Mech.* **51**, 497–512.
- O'MALLEY, B. 1967 The first boundary value problem for certain linear elliptic differential equations involving two small parameters. *Arch. Rat. Mech. Anal.* **26**, 68–82.
- RHODE, W. S. 1971 Observations of the vibration of the basilar membrane in squirrel monkeys using the Mössbauer technique. *J. Acoust. Soc. Am.* **49**, 1218–1231.
- ROBLES, L., RHODE, W. & GEISLER, C. D. 1976 Transient response of the basilar membrane measured in squirrel monkeys using the Mössbauer effect. *J. Acoust. Soc. Am.* **59**, 926–939.
- STEELE, C. R. & TABER, L. A. 1979 Comparison of WKB calculations and experimental results for three-dimensional cochlear models. *J. Acoust. Soc. Am.* **65**, 1007–1018.
- VOLDRICH, L. 1978 Mechanical properties of the basilar membrane. *Acta Otolaryng.* **86**, 331–335.